NONINVASIVE MAPPING OF THE SPINAL CANAL HYDRODYNAMIC COMPLAINCE USING BOND GRAPH TECHNIQUE AND MAGNETIC RESONANCE IMAGING

Naresh Yallapragada, Noam Alperin

Department of Radiology,
University of Illinois at Chicago,
Chicago, IL

INTRODUCTION

The aim of this paper is to present a noninvasive method for quantifying the spinal canal hydrodynamic compliance from Magnetic Resonance Imaging (MRI) measurements of volumetric cerebrospinal fluid (CSF) flow. The spinal canal compartment contributes to the overall compliance of the craniospinal system. Thus it plays an important role in regulating craniospinal hydrodynamics and intracranial pressure. Limited information is available on the range of spinal canal compliance values in humans. Even less is known about the distribution of the compliance along the spinal canal, in the healthy and the diseased states, as current methods require injection of fluid into the CSF spaces and thus are associated with risk and morbidity [1].

The proposed method estimates the spinal canal compliance using measurements of the oscillatory CSF flow dynamics at several locations with motion-sensitive MRI technique and thus is non-invasive. The relationship between the volumetric CSF flow rates at different spinal canal locations was used to construct a mathematical model using the Bond Graph technique [2]. The Bond Graph technique is a graphical tool for representing the energy flow using causal relationships and for deriving the equations governing the dynamics of state-determined systems.

METHODS

The Bond Graph model of the spinal canal hydrodynamics provides a graphical description of energy process associated with the flow of the CSF in this compliant conduit. Our model accounts for energy storage and dissipation processes associated with CSF space compliance and CSF inertia, and flow resistance, respectively. These physical properties are distributed along the length of the spinal canal. The model lumps these distributed parameters into finite number of sub-segments to obtain a state-determined system. This lumped parameter model comprises of interleaved compliant and rigid segments.
The Bond Graph representation of our spinal canal model is shown in Figure 1, where a_i, I_i and R_i are the volumetric CSF flow rate, CSF inertia, and flow resistance in the rigid segment 'i', respectively, and, P_{ij} and C_{ij} are the pressure and the compliance in the compliant segment 'ij', respectively.

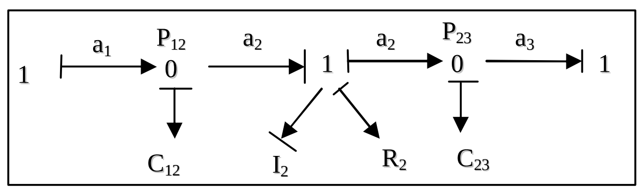

Figure 1. Bond Graph representation of the spinal canal hydrodynamic model.

The differential equations governing the CSF flow were derived from Bond Graph representation and are as follows.

$$\frac{dP_{12}}{dt} = (a_1 - a_2)/ C_{12} \qquad (1)$$

$$\frac{da_2}{dt} = (- R_2 * a_2 + P_{12} - P_{23})/ I_2 \qquad (2)$$

$$\frac{dP_{23}}{dt} = (a_2 - a_3)/ C_{23} \qquad (3)$$

The oscillating CSF flow rates rates in different segments at different locations (a1, a2 and a3) along the spinal canal were measured with a velocity encoded MRI technique, the cine phase-contrast MRI. The technique yields time series maps of velocities through the imaged plane from which volumetric flow rate is calculated. Flow dynamics satisfying the differential equations are then compared iteratively with actual flow measurements to yield compliance, resistance and inertia. Discrete-time state space tools were employed to expedite the flow calculations [3].

Four in a healthy volunteers were scanned with a 1.5T MRI scanner (GE Medical system, Milwaukee, WI) to obtain volumetric CSF flow measurements at six different locations along the spinal canal. Validation of the model consistency was obtained by comparing the overall compliance of a large segment of the spinal canal to the sum of its several sub-segments calculated independently.

RESULTS

Volumetric CSF flow waveforms measured at six different locations in one of the four subjects are shown in Figure 2. The location of the measurements in millimeter is indicated in the graph.

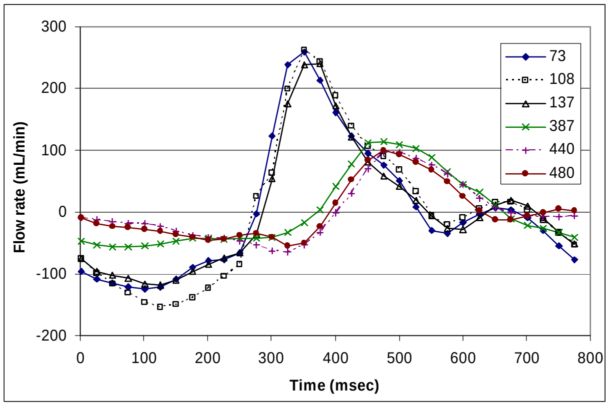

Figure 2. Measured volumetric CSF flow waveforms used to calculate the compliance distribution.

Anatomical and CSF velocity encoded images at 2 different locations along the spinal canal for this subject are shown in Figure 3. The calculated hydrodynamic compliance values of different segments and segment combination along the spinal canal of this subject are summarized in Figure 4.

The total compliance of the spinal canal in the four healthy volunteers ranged from 1.7 mL/mmHg to 45.2 mL/mmHg. The middle and the lower segments of the spinal canal contributed the majority of the spinal canal compliance. Consistency was found between the overall compliance of a large segment and the sum of its several sub-segments calculated independently.

CONCLUSIONS

MRI-derived CSF velocity measurements and Bond Graph methodology were introduced to quantify noninvasively the spinal canal hydrodynamic compliance and its distribution. Results show that the main contribution to the overall compliance is from the thoracic and lumbar sections. These results are consistent with the fact that the dura mater membrane is more confined by the spinal column at the cervical region than the rest of the spinal canal. In addition, the consistency of compliance values derived independently for the different combination of the segments of the canal further supports the validity of the proposed methodology.

The proposed method utilizes the dynamics of the pulsatile CSF flow occurring naturally during the cardiac cycle, rather than altering the state by external intervention, as a means to characterize the mechanical parameters governing the steady state system dynamics.

The method may provide an important tool to improve our understanding of the role of the spinal canal in regulating the complex dynamics associated with the craniospinal system. The new method is safe and thus can be used to study the healthy and the diseased states. The proposed method could become a practical diagnostic tool since a patient's specific characterization of the spinal canal hydrodynamics would be computed in few minutes.

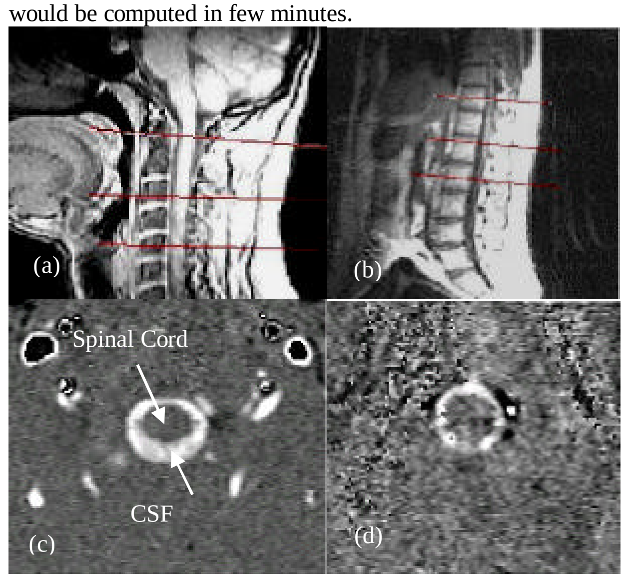

Figure 3. Anatomical images of the upper (a) and lower (b) portions of the spinal canal. Superimposed are the locations of the CSF flow measurements. Below are the velocity-encoded images acquired during the systolic phase of the cardiac cycle from a cervical region (c) and a lumbar region (d), respectively.

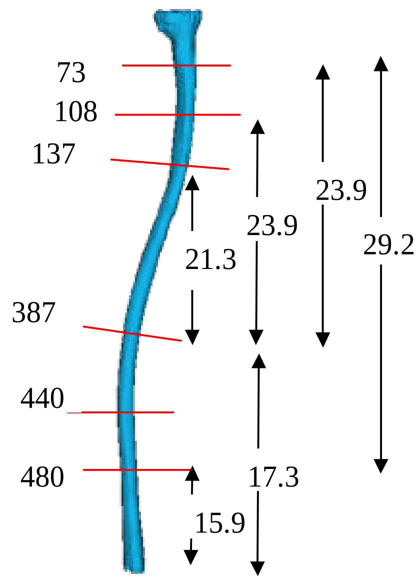

Figure 4. Calculated hydrodynamic compliances in units of mL/mmHg for segments distributed along the spinal canal.

REFERENCES

1. Marmarou, A, Shulman, K, and LaMorgese J, "Compartmental analysis of compliance and outflow resistance of the cerebrospinal fluid system." J Neurosurg; 1975; 43; p 523-534.
2. Karnopp, DC, Margolis, DL, and Rosenberg, RC, "System Dynamics: Modeling and Simulation of Mechatronic Systems", IIIrd Ed., John Wiley and Sons, Inc., 2000.
3. Franklin, GF, Powell, JD, and Workman, ML, "Digital Control of Dynamic Systems", IIIrd Ed., Addison-Wesley, 1998.